CP845, *Shock Compression of Condensed Matter - 2005,*
edited by M. D. Furnish, M. Elert, T. P. Russell, and C. T. White

POST-SHOCK TEMPERATURE AND FREE SURFACE VELOCITY MEASUREMENTS OF BASALT

S. T. Stewart[1], G. B. Kennedy[1], L. E. Senft[1], M. R. Furlanetto[2], A. W. Obst[2], J. R. Payton[2], and A. Seifter[2]

[1]*Department of Earth and Planetary Sciences, Harvard University, 20 Oxford Street, Cambridge MA 02138*
[2]*University of California, Los Alamos National Laboratory, Physics Division, P-23, Los Alamos, NM 87545*

Abstract. Basalt is the most common rock type on planetary surfaces. Post-shock temperature and particle velocity measurements constrain the equation of state of basalt and provide fundamental information about the outcome of planetary impact events. A high-speed, infrared, four-wavelength pyrometer, developed at Los Alamos National Laboratory (LANL), is used with customized front end optics at the Harvard Shock Compression Laboratory for concurrent observations of particle velocity and free surface thermal emission. In an experiment on Columbia River basalt released from a peak shock pressure of 28.9±0.2 GPa, the apparent post-shock temperature is wavelength dependent. The 3.5 and 4.8-μm channels record apparent temperatures between 605 and 630 K, using an emissivity range of 0.7-1.0. The 1.8 and 2.3-μm channels record apparent temperatures of ~700 K and ~800 K, respectively. The pyrometry data are well fit by a two component temperature distribution: (1) a predominantly 565-610 K free surface, in good agreement with the 570 K predicted by the basalt EOS in the shock physics code CTH, and (2) a small area fraction of 1700-2000 K hot spots. The model is in good agreement with inferred basaltic meteorite hot spot temperatures; however, the hot spot model is not unique. Free surface velocity measurements are slower than predicted by CTH, indicating a steeper release path than in the model equation of state.

Keywords: Post-shock temperature, basalt, equations of state, pyrometry, VISAR, CTH
PACS: 62.50.+p, 91.60.Fe, 07.20.Ka, 83.80.Nb

INTRODUCTION

Shock temperature data are necessary to investigate a wide range of problems in the earth and planetary sciences, including phase changes during impact events, the temperature field surrounding fresh impact craters, and the thermal history of meteorites. The post-shock temperatures of rocks and minerals provide strong constraints on their equations of state. Multi-wavelength data also furnish insights into the heterogeneities of shock processes in natural materials.

Most previous shock temperature studies have utilized optical pyrometry to observe high (typically, >1500 K) peak shock temperatures in transparent minerals and liquids or high post-shock temperatures in metals and minerals. Infrared pyrometry allows investigation of shock processes at lower pressures. Furthermore, in many natural materials, hysteretic release isentropes significantly complicate the calculation of post-shock temperatures, as demonstrated by the first study of low post-shock temperatures in minerals [1].

We have begun a new study of post-shock temperatures (in the range ~400-1500 K) in metals [2], rocks, and minerals. Here we present preliminary results from simultaneous measurements of particle velocity and near-infrared

free surface emission from shocked basalt.

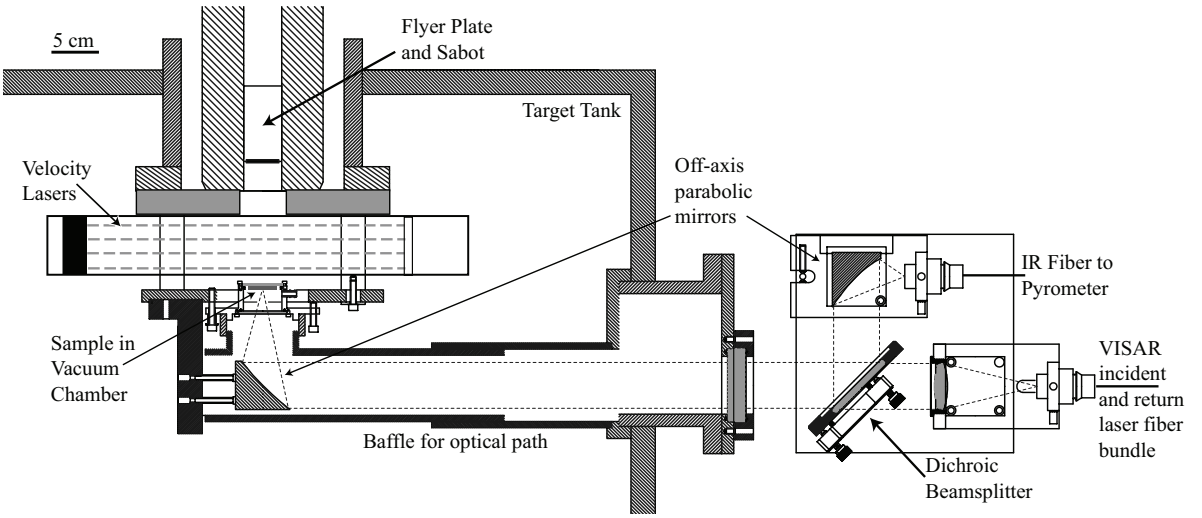

FIGURE 1. Plan view of experimental configuration for simultaneous pyrometer and VISAR measurements on the Harvard 40-mm gun. An off-axis parabolic mirror collects and collimates radiance emitted from a ~4-mm diameter spot on the downrange face of the sample, as well as focusing the incident and collecting the reflected laser light for the VISAR. The collimated light is split with a >1200 nm reflecting dichroic beamsplitter between the IR pyrometer and the visible (532 nm) VISAR. The optical path is enclosed in light-tight tubing to shield from propellant gases during the experiment.

EXPERIMENTAL PROCEDURE

Planar shock waves with peak pressures up to ~35 GPa are generated in basalt using the 40-mm single stage powder gun in the Harvard Shock Compression Laboratory [3]. A Ø34×3 mm molybdenum flyer plate impacts a 2-mm thick aluminum-2024 driver plate, which also seals a small aluminum vacuum chamber containing the basalt specimen (Fig. 1). The sample vacuum chamber is purged with He gas and evacuated to <0.5 millitorr, eliminating any background emission from gas in the chamber. A 1-cm diameter aperture was placed behind the basalt sample to shield the pyrometer from any emission from the edges of the driver plate and from reflections off the walls of the vacuum chamber.

Concurrent particle velocity and radiance measurements from the same location on the downrange, free surface of the basalt are achieved using a shared optical system [see description in 2]. Free surface particle velocity is measured with a VALYN VISAR. The radiance is delivered to a high-speed, infrared, four-wavelength (1.8, 2.3, 3.5, 4.8 μm) pyrometer with InSb detectors via a 1-mm diameter chalcogenide C2 infrared fiber, and detector voltage is recorded on 12-bit 100 MHz digitizers [4]. The pyrometer is sensitive to radiance temperatures as low as 400 K and has a temporal resolution of ~17 ns. The system is calibrated with a Mikron M360 black body source that was observed with the same optics and fibers as used in the experiments. The calibrated radiation temperature is converted to an apparent temperature for each channel using the emissivity of the sample. If the apparent temperature of all four channels overlap, as in the case of our validation experiments on aluminum 2024 [2], then the apparent temperature is considered to be the true temperature of a homogeneous surface.

The Columbia River flood basalt (CRB) specimens, from Snake River Valley near Clarkston, WA ($\langle\rho\rangle$=2.83±0.10 g/cm3, $\langle V_P\rangle$= 5.73±0.28 km/s, $\langle V_S\rangle$=3.46±0.04 km/s), are cored and cut from hand samples into nominally Ø34×2 mm discs. The basalt and driver plate are lapped plane parallel with 15 micron diamond grit and hand polished to an optical (~100 nm) finish using 58-nm alumina powder polish. The basalt is affixed to the driver plate using a ~10 μm layer of Loctite 326 epoxy. No macroscopic pores intersect the free surface. The observed area, a ~4-mm diameter spot

for the pyrometer and ~1-mm diameter spot for the VISAR, contains microscopic pores that are typically several 10s μm across.

RESULTS AND DISCUSSION

The apparent temperature of basalt released from a peak shock pressure of 28.9±0.2 GPa (impact velocity of 2.24±0.01 km/s) is shown in Fig. 2. By applying an emissivity range between 0.7 and 1.0 for basalt [5], we determine the range of apparent temperatures, indicated by the thickness of the data traces. There is a small temperature excursion at the time of shock breakout, which is seen in previous post-shock temperature measurements on metals and minerals [1, 2, 6]. The two longest wavelength channels are in good agreement, with a constant temperature following the breakout. The two shortest wavelength channels record significantly higher temperatures that increase with time.

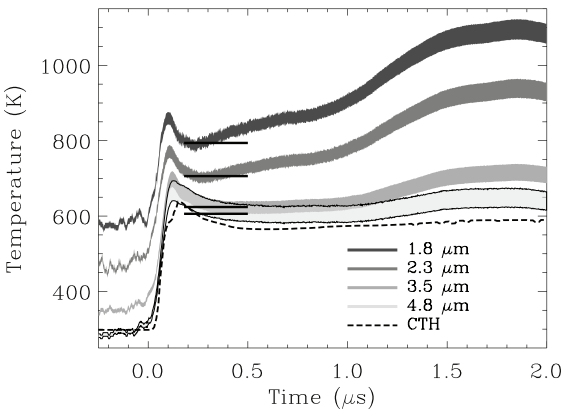

FIGURE 2. Multi-wavelength post-shock temperature measurements on basalt released from a peak shock pressure of 28.9 GPa, assuming an emissivity range of 0.7-1.0. Horizontal bars indicate the apparent temperature at each detector wavelength for a two-component temperature surface model described in the text. Inferred 565-610 K surface temperatures are in good agreement with free surface temperatures from a simulation of the experiment using the CTH basalt EOS.

The high apparent temperatures in the 1.8 and 2.3 μm channels cannot be reconciled by varying the emissivity as a function of wavelength. We interpret the discrepancy between the shorter and longer wavelengths to be evidence for hot spots in the field of view. We fit a simple two-component model to the data, where the radiance, L, at each wavelength, λ, is described by an apparent temperature, T', given by Planck's Law,

$$L_\lambda(T') = \varepsilon' \frac{2hc^2}{\lambda^5 (e^{hc/(\lambda k T')} - 1)}.$$

Here, ε is emissivity, h is Planck's constant, c is the speed of light, and k is Boltzmann's constant. If a surface with temperature, T_S, has a small area fraction, α, of hot spots with temperature, T_{HS}, then the radiance is the sum of two components,

$$L_\lambda(T') = (1-\alpha)\varepsilon_S \frac{2hc^2}{\lambda^5 (e^{hc/(\lambda k T_S)} - 1)} + \alpha \varepsilon_{HS} \frac{2hc^2}{\lambda^5 (e^{hc/(\lambda k T_{HS})} - 1)}.$$

Hence, the apparent temperature is defined by

$$T' = \frac{hc}{\lambda k \ln\left[\frac{1}{\frac{1-\alpha}{e^{hc/(\lambda k T_S)} - 1} + \frac{\alpha}{e^{hc/(\lambda k T_{HS})} - 1}} + 1\right]},$$

assuming the emissivities are equal. The long wavelength channels constrain the surface temperature between 565 and 610 K. The data are well fit by a ~590 K surface with hot spots in the temperature range of 1700 to 2000 K occupying an area fraction of 0.45 to 0.25%, respectively. The model apparent temperature at each wavelength is shown by the horizontal bars in Fig. 2.

To produce 1700-2000 K hot spots, some material must reach the melting point. The 28.9 GPa experiment is well below the pressure required for bulk melting for basalt, and the results are consistent with localized melting in shear bands or fractures [7] or at grain boundaries between different impedance minerals [8]. The inferred hot spot temperatures are in excellent agreement with petrographic studies of localized melting in basaltic meteorites from Mars shocked to similar pressures [8]. However, the measured surface temperature of CRB is about 100 K higher than the bulk rock post-shock temperature inferred for the same meteorites.

The two-component model probably underestimates the area fraction of hot spots. The model fit is dominated by the hottest spots, and a hot spot temperature distribution with the inferred peak temperature could also satisfy the data.

The free surface particle velocity provides information about the pressure-volume release path from the peak shock state. The free surface particle velocities, for basalt subject to peak shock pressures between 2.0 and 32.0 GPa, are shown in Fig. 3. Each experiment is modeled with the CTH shock physics code using the standard equation of state SESAME tables for the molybdenum flyer, aluminum 2024 driver, and basalt. The results are compared to the observed temperatures and particle velocities (Figs. 2-3, dashed lines). In general, the observed free surface particle velocities are lower than the calculations, indicating that the release path is steeper compared to the model EOS.

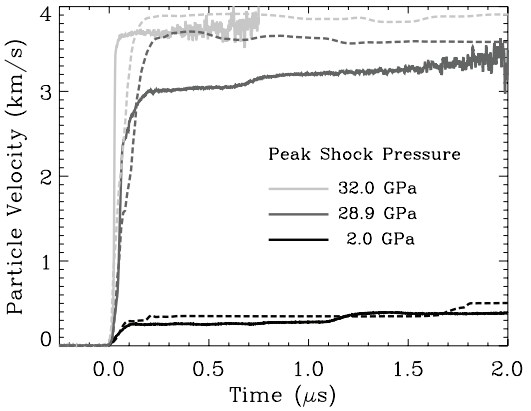

FIGURE 3. Measured (solid) and modeled (dashed) free surface velocities of basalt shocked to peak pressures of 2.0, 28.9 and 32.0 GPa.

CONCLUSIONS

New shock experiments on basalt provide fundamental information required to improve EOS models. Here we present the first post-shock temperature data on basalt, which provides insight into the distribution of temperatures following impact events. Our data quantify the heterogeneity that arises from pre-existing pores and fractures and/or the effect of mixing materials with different shock impedances. New EOS models will aid in calculations of post-impact conditions on Mars [9], the thermal history of meteorites [10], and conditions for melting subsurface ice [11]. Heterogeneous shock pressures and temperatures are observed around terrestrial craters and in meteorites. Understanding the effect of heterogeneities on the temperature distribution following impact events will aid in the interpretation of meteorites, terrestrial field studies, and simulating impact events on Mars.

ACKNOWLEDGEMENTS

Funding was provided by NASA grant #NNG04GD17G.

REFERENCES

1. Raikes, S. A. and T. J. Ahrens, "Post-shock temperature in minerals," *Geophys. J. R. Astr. Soc.* **58**, 717-747 (1979).
2. Seifter, A., et al., "Post-shock Temperature Measurements of Aluminum," in *Shock Compression of Condensed Matter -- 2005*, edited by M. Furnish, AIP, 2005, pp. TBD.
3. Stewart, S. T., "The Shock Compression Laboratory at Harvard: A New Facility for Planetary Impact Processes," *Proc. Lunar & Planet. Sci. Conf.* **XXXV**, Abs. 1290 (2004).
4. Boboridis, K., A. Seifter, and A. W. Obst, "High-Speed infrared pyrometry for surface temperature measurements on shocked solids," *VDI-Bericht* **1784**, 119-126 (2003).
5. Burgi, P.-Y., M. Caillet, and S. Haefeli, "Field temperature measurements at Erta'Ale Lava Lake, Ethiopia," *Bull. Volcanol.* **64**, 472-485 (2002).
6. Seifter, A., et al., "Low-Temperature Measurements on Shock-Loaded Tin," *26th Intl. Congr. High-Speed Photo. & Photonics* **5580**, 93-105 (2004).
7. Miller, P. J., C. S. Coffey, and V. F. DeVost, "Heating in crystalline solids due to rapid deformation," *J. Appl. Phys.* **59**, 913-916 (1986).
8. Stoffler, D., et al., "Shock metamorphism and petrography of the Shergotty achondrite," *Geochim. Cosmochim. Acta* **50**, 889-903 (1986).
9. Pierazzo, E., N. A. Artemieva, and B. A. Ivanov, "Starting conditions for hydrothermal systems underneat Martian craters: Hydrocode modeling," *Proc. Lunar & Planet. Sci. Conf.* **XXXV**, 1352 (2004).
10. Artemieva, N. and B. Ivanov, "Launch of martian meteorites in oblique impacts," *Icarus* **171**, 84-101 (2004).
11. Stewart, S. T., J. D. O'Keefe, and T. J. Ahrens, "Impact processing and redistribution of near-surface water on Mars," in *Shock Compression of Condensed Matter -- 2003*, edited by M.D. Furnish, et al., American Institute of Physics, Melville, NY, 2004, pp. 1484-1487.